SENSOR LOCATION EFFECT ON FLEXIBLE ROBOT STABILITY ANDCONTROL

Department of Mechanical and Aerospace Engineering,
Carleton University, Ottawa, Ontario, K1S 5B6.

Abstract: The effect of sensors located at different points on a flexible robot is simulated using nonadaptive and fuzzy logic system (FLS) adaptive control strategies. Collocated joint encoders fail to capture nonminimum phase (NMP) response while noncollocated position sensors capture NMP response but cause control action delays. A feedback loop time delay simulates NMP response and a forward loop time delay provides corrective control action. Results demonstrate stability for all trajectories obtained with encoders collocated at the robot joints, a position sensor noncollocated at the end effector then with the sensor located at 2.25m from the end effector.

Keywords: Flexible Robot, Sensors, Inverse Dynamics, Adaptive Control, Fuzzy Logic

1. INTRODUCTION

Structural flexibility is one of the most important factors causing significant difficulty during operational control of space robots, especially, position control. This paper presents the results of tracking a square trajectory 12.6m x 12.6m by a two-link flexible robot with sensors located at different positions. Elastic vibrations of robot links coupled with rotating nonlinear dynamics presents a complex challenge for control. Sensor location adds complexity to accurately detecting and controlling end effector positions. Results are obtained for nonadaptive and fuzzy logic system (FLS) adaptive control strategies. For each strategy simulations are performed for three cases; 1. a rotation encoder collocated at the elbow joint; 2. a position sensor located at the end effector; 3. the position sensor relocated to 2.25m from the end effector.

Banerjee and Singhose (1998) used an input shaping method coupled with inverse kinematics and a recursive order-n algorithm control scheme for both linear and nonlinear control laws to control a two-link flexible robot and reduce residual vibrations. Sasiadek and Srinivasan (1989) applied model reference adaptive control (MRAC) with a modal expansion of the first three vibration modes to control position and vibration of a single-link flexible robot. They further reduced errors and decreased settling time of transient responses to step inputs. The use of fuzzy logic to control robots has produced good results (de Silva 1995, Green and Sasiadek 2004a, b, 2005). The effect of a sensor located at the end effector on robot control is given in a previous study (Green and Sasiadek, 2004c).

2. ROBOT DYNAMICS

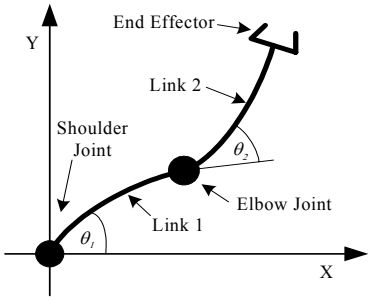

Fig.1. Flexible Robot.

The two-degree-of-freedom (2-dof) flexible robot shown in Figure 1 has planar motion and vibration modes. Gravity and friction effects are omitted for space borne operation. It is revolute about the shoulder and elbow joints. Each link has length L = 4.5 m with mass density ρ = 0.335 kg/m and flexural rigidity EI = 1676 N-m^2 taken from Banerjee and Singhose (1998).

2.1 Rigid Dynamics

The nonlinear rigid-link dynamics of a multilink robot is derived in Euler-Lagrange form in terms of kinetic and potential energies. For an independent set of generalized coordinates, $q_i = q_1,.....,q_n$, the total kinetic and potential energies, T and U, stored in the system is defined by the Lagrangian (Thomson, 1981).

$$\mathcal{L}\left(q_i, \dot{q}_i\right) = T - U, \qquad i = 1,.....,n \qquad (1)$$

For a generalized force F_i acting on a generalized coordinate q_i the dynamic equations of motion are given by.

$$\frac{d}{dt}\frac{\partial \mathfrak{L}}{\partial \dot{q}_i} - \frac{\partial \mathfrak{L}}{\partial q_i} = F_i, \qquad i = 1,.....,n \tag{2}$$

Kinetic energy is given by.

$$T = \frac{1}{2}\sum_{i=1}^{n}\sum_{j=1}^{n} M_{ij}\dot{q}_i\dot{q}_j, \tag{3}$$

For space robot applications gravity potential energy is zero, U is omitted and the Euler-Lagrange rigid dynamics matrix equations are given by (Green and Sasiadek, 2004b).

$$\boldsymbol{\tau} = \mathbf{M}(\theta)\ddot{\theta} + \mathbf{C}(\dot{\theta},\theta)\dot{\theta} \tag{4}$$

2.2 Flexible Dynamics

Extensive work has been published on the dynamics and control of flexible robots using assumed modes (Fraser and Daniel 1991; Green and Sasiadek 2004a, b, c, 2005; De Luca and Siciliano 1991; Sasiadek and Srinivasan 1989). For an Euler-Bernoulli beam with uniformly distributed load *p(x,t)* and flexural rigidity *EI*, the equation of motion is given by.

$$\partial^2/\partial x^2\left(EI\,\partial^2 u(x,t)/\partial x^2\right)dx + m(x)\,\partial^2 u(x,t)/\partial t^2 = p(x,t) \tag{5}$$

The normal modes $\phi_i(x)$ must satisfy the equation.

$$\left[EI\phi_i''(x)\right]'' - \omega_i^2 m(x)\phi_i(x) = 0 \tag{6}$$

and its boundary conditions given by.

$$\phi_i(0) = \phi_i'(0) = 0; \quad \phi_i''(L) = \phi_i'''(L) = 0$$

The solution to (5) is an approximate deformation of an elastic beam subjected to transverse vibrations given by (Thomson, 1981; Fraser and Daniel, 1991).

$$u(x,t) = \sum_{i=1}^{n}\phi_i(x)q_i(t) \tag{7}$$

where; $\phi_i(x)$ are assumed mode shapes. Assumed modes of vibration for an Euler-Bernoulli cantilever beam are coupled with rotating links to model the two-link flexible robot and capture its nonlinear multibody interactions. This approach accommodates configuration changes during operation, whereas, normal modes must be continually recomputed (Fraser and Daniel, 1991). The dominant assumed mode of vibration is used to form an Euler-Lagrange inverse flexible dynamics robot model. Cantilever assumed mode shapes are given by transverse beam vibration theory (Thomson, 1981).

$$\phi_{ci}(x) = A[\cosh\lambda_{ci}x - \cos\lambda_{ci}x - k_{ci}(\sinh\lambda_{ci}x - \sin\lambda_{ci}x)] \tag{8}$$

where; $A = 0.1$ is an arbitrary constant, $\lambda_{ci}L = (i - 0.5)\pi$, $i = 1,..,n$ are numerically approximated roots of the characteristic equation $\cos(\lambda_{ci}L)\cosh(\lambda_{ci}L) + 1 = 0$ and $k_{ci} = \cos\lambda_{ci}L + \cosh\lambda_{ci}L / \sin\lambda_{ci}L + \sinh\lambda_{ci}L$.
Modal frequencies are given by.

$$\omega_{ci} = (\lambda_{ci}L)^2\sqrt{EI/\rho L^4} \tag{9}$$

Proportional and derivative (PD) gains for the dominant assumed mode are given by.

$$\mathbf{K_p} = \mathrm{diag}\left[\omega_{c1}^2 \quad \omega_{c1}^2\right] = \mathrm{diag}\left[150.79 \quad 150.79\right] \tag{10}$$

$$\mathbf{K_d} = \mathrm{diag}\left[2\zeta\omega_{c1} \quad 2\zeta\omega_{c1}\right] = \mathrm{diag}\left[17.364 \quad 17.364\right] \tag{11}$$

for $\omega_{c1} = 12.28$ Hz and damping ratio $\zeta = 0.707$.

The deformation $u(x,t)$ in (7) is substituted into the Euler-Lagrange dynamics to derive elastic kinetic and potential energies given by.

$$T_e = 1/2\left(\sum_i^n\sum_j^n \dot{q}_i\dot{q}_j\int_0^L \phi_i\phi_j m(x)dx\right) \tag{12}$$

$$U_e = 1/2\left(\sum_i^n\sum_j^n \dot{q}_i\dot{q}_j\int_0^L EI\phi_i''\phi_j''dx\right) \tag{13}$$

Combining rigid and flexible terms the matrix equations are given by (Green and Sasiadek, 2004b).

$$\boldsymbol{\tau} = \mathbf{M}(\mathbf{q})\ddot{\mathbf{q}} + \mathbf{C}(\dot{\mathbf{q}},\mathbf{q})\dot{\mathbf{q}} + \mathbf{K}\mathbf{q} \tag{14}$$

Matrices M comprise rigid and flexible link elements, **C** only rigid Coriolis and centrifugal terms and **K** is a stiffness matrix. The generalized coordinate vector **q** comprises joint angles and link deformations. End effector and joint masses, robot task forces and payloads are excluded whereas link masses are included. Assumed modes are computed on the assumption of small elastic deformation where second-order terms of interacting elastic modes can be neglected and with orthogonality simplify (14). Omitting elastic Coriolis and centrifugal components gives the rigid dynamics coupling matrix. Beres and Sasiadek (1995) published a complete derivation for n-dof manipulator dynamics.

3. SENSOR LOCATION, NONMINIMUM PHASE RESPONSE AND STABILITY

Nonminimum phase (NMP) response is an inherent problem with flexible robot control. When torque actuates a robot joint it induces flexing and momentary acceleration of the end effector in a direction opposite in sense to that commanded by the torque. Analytical control theory describes this behaviour by transfer function poles or zeros occurring in the right-half s-plane and termed a phase shift or, transport lag, between the actuator and end effector. For continuous systems this phase shift creates a time delay between end effector position and control action needed to correct position errors and corresponds to the time for mechanical wave propagation through the link from joint to end effector.

Closely associated with NMP response is the distance between sensor and actuator, or noncollocation. This causes time delays in joint control actuation in response to position errors computed using data fed back from a sensor located at the end effector. Collocated control provides joint actuation in response to joint angle data from an encoder located at the joint. Typically, collocated control is suitable for fixed-base rigid-link robots operating at speeds where flexibility is insignificant and noncollocated sensors do not experience NMP response.

When a rotation encoder is collocated with a joint actuator on a flexible robot it is considered a *hyperstable* system. Hyperstable systems require; equal number of sensors and actuators; sensor and actuator types match; and sensor/actuator collocation. However, these conditions detract from proper control being applied to flexible robots. For a single (dominant) mode of vibration the flexible robot given by (14) with noncollocated sensors is evaluated as stable by the Routh-Hurwitz criterion, (Stieber, Vukovich and Petriu 1997).

An operational space control strategy, shown in Figure 4, is used to simulate noncollocated control where joint angles and rates transform through direct kinematics equations into end effector positions and velocities. NMP responses for sensors located at the end effector and 2.25m along link 2 are modeled using time delays between the sensor and joint 1 in the feedback loop. Transport delay blocks (not shown) with a second-order Padé approximation are included in Matlab/Simulink™ simulation models. NMP response is corrected by a time delay in commanded inputs to coincide with the delayed feedback positions and to ensure accurate computation of the control law. Time delays are calculated using the transverse beam vibration wave velocity c (Alexander 1988, Thomson 1981) given by.

$$c = \sqrt{\frac{E}{\rho}} = \sqrt{\frac{1745833}{21}} = 288.33 \text{ m/s} \quad (15)$$

Delay time from joint 1 to the end effector for two link lengths, i.e. 9m, is given by.

$$t_{d_1} = \frac{9}{288.33} = 0.0312\text{s} \quad (16)$$

Delay time from joint 2 to the end effector for one link length of 4.5m is given by.

$$t_{d_2} = \frac{4.5}{288.33} = 0.0156\text{s} \quad (17)$$

Average trajectory simulation time is 402s for 16000 simulation steps (ss) at 0.001 step size, i.e. 0.0252s per step. Simulation delay times from joint 1 and joint 2 to the end effector are.

$$d_1 = \frac{0.0312}{0.0252} = 1.238\text{ss} \quad (18)$$

and

$$d_2 = \frac{0.0156}{0.0252} = 0.619\text{ss} \quad (19)$$

Similarly, delay times and simulation steps for the sensor located 6.75m from joint 1 and 2.25m from joint 2 are 0.0234s (0.9289ss) and 0.0078s (0.3097ss) respectively. For simulation, time delays d_1 and 0.9289ss for a sensor noncollocated at the end effector and at 6.75m from joint 1 respectively are implemented in the control feedback loop.

4. CONTROL STRATEGIES

4.1 Nonadaptive Control

Nonadaptive control is that shown in Figure 4 excluding the FLS. Commanded x_c and y_c end effector positions input to the control system and summing with feedback values form position and velocity errors. PD gains $\mathbf{K}_\text{p}$ and $\mathbf{K}_\text{d}$ operate on these errors to compute the Jacobian transpose control law.

$$\boldsymbol{\tau} = \mathbf{J}^\text{T}(\theta)\left[\mathbf{K}_\text{p}\begin{pmatrix} e_x \\ e_y \end{pmatrix} + \mathbf{K}_\text{d}\begin{pmatrix} \dot{e}_x \\ \dot{e}_y \end{pmatrix}\right] \quad (20)$$

Control of a flexible robot is compounded by link vibration and an effective strategy must be able to suppress residual vibrations to achieve tracking accuracy.

4.2 Fuzzy Logic System Adaptive Control

The FLS adaptive control strategy is shown in Figure 4. Adaptive control is achieved with fuzzy output variable λ determined in the FLS by elastic link deformation inputs, δ_1 and δ_2, fed back from the flexible dynamics and operates on (15) to give (16).

$$\tau = K_s \lambda \left\{ \mathbf{J}^{T}(\theta) \left[\mathbf{K}_p \begin{pmatrix} e_x \\ e_y \end{pmatrix} + \mathbf{K}_d \begin{pmatrix} \dot{e}_x \\ \dot{e}_y \end{pmatrix} \right] \right\} \qquad (21)$$

Verbal descriptors for positive (P), positive medium (PM), positive maximum (PMAX), zero (ZERO), and negative (N) are used for the membership functions (MFs) shown in Figs. 2 and 3 that generate nine fuzzy rules of the form;

IF δ_1 is N AND δ_2 is P THEN λ is PMAX

The FLS is developed intuitively, such that, as each link deforms positively or negatively they complement or counter deformation of the other. Then λ varies according to the magnitude of resultant deformation and ranges from ZERO for zero deformation to PMAX for the largest deformation, thereby, forming a symmetric fuzzy rule matrix given in Table 1.

The universes of discourse range from -5 m to 5 m for δ_1 and δ_2 and 0 to 1.0 for λ as shown in Figures 2 and 3. Values of δ_1 and δ_2 are normalized by gain $K_n = 5$ before input to the FLS. An FLS scaling gain K_s operates on the λ MFs to modify their base widths and provides improved tracking accuracy as K_s is increased. An optimal FLS is based on three MFs for each input and output variable with $K_s = 15$ (Green and Sasiadek, 2004a).

Table 1 Fuzzy logic system rule matrix for three triangular membership functions (9 rules).

		δ_2		
		N	ZERO	P
	λ			
δ_1	N	PMAX	PM	PMAX
	ZERO	PM	ZERO	PM
	P	PMAX	PM	PMAX

5. SIMULATION RESULTS

Figures 5 to 8 show tracking clockwise starting at lower left. Results for a sensor collocated, noncollocated at the end effector (NMP) and NMP corrected are shown superposed for nonadaptive and FLS adaptive control in Figures 5 (a) and (b). Large overshoots occurr at each direction switch for nonadaptive control but a marked reduction in transient overshoot amplitudes is achieved with FLS adaptive control. Zoomed transients at direction switches are shown in Figures 6 (a) and (b). A decrease in overshoot amplitude is evident for NMP with nonadaptive control at the second direction switch but is the reverse for the rest of the trajectory. An increase in overshoot is experienced with FLS adaptive control. But, NMP correction has minimal effect in both cases with a slight increase in amplitude. Results for the sensor located at 2.25 m along link 2 given in Figures 7 (a) and (b) show minimal difference. The effect of NMP correction is small for both control strategies as shown in Figures 8 (a) and (b). However, the collocated trajectory intersects with the noncollocated trajectories in Figure 8 (a) whereas; they do not intersect in Figure 8 (b) because of the reduced transient amplitudes achieved with FLS adaptive collocated control. Simulation times are 14 min 29 sec for nonadaptive and 20 min 21 sec for FLS adaptive control.

6. CONCLUSION

FLS adaptive control significantly reduces tracking errors and overcomes the complexities of a flexible robot and limitations of classical control. FLS adaptive control maintains overriding effectiveness on tracking control regardless of sensor location. Stability is maintained for all sensor locations but more significantly, accuracy is preserved using FLS adaptive control with a noncollocated sensor at the end effector despite hyperstability constraints.

REFERENCES

Alexander H.L. (1988). Control of Articulated and Deformable Space Structures. In: *Machine Intelligence and Autonomy for Aerospace Systems*, (E. Heer and H. Lum, Ed), pp. 327-347 AIAA Progress in Astronautics and Aeronautics, AIAA, Washington, DC.

Banerjee, A.K. and W. Singhose (1998). Command Shaping in Tracking Control of a Two-Link Flexible Robot. *AIAA Journal of Guidance Dynamics and Control*, **21**, Engineering Note, 1012-1015.

Beres, W. and J.Z. Sasiadek (1995). Finite Element Dynamic Model of Multi-link Flexible Manipulators, *Applied Mathematics and Computer Science,* **5**, 231-262.

De Luca, A. and B. Siciliano (1991). Closed-Form Dynamic Model of Planar Multilink Lightweight Robots, *IEEE Transactions on Systems, Man and Cybernetics*, **21**, 826-839.

de Silva, C.W. (1995). *Intelligent Control: Fuzzy Logic Applications,* CRC Press, Boca Raton, FL.

Fraser, A.R. and R.W. Daniel (1991). *Perturbation*

Techniques for Flexible Manipulators, The Kluwer International Series in Engineering and Computer Science, **138**, Kluwer, Dordrecht, Netherlands.

Green, A. and J.Z. Sasiadek (2004a). Optimal Fuzzy Controller for a Flexible Robot. In: *Proceedings of the AIAA Guidance, Navigation and Control* Conference, Reston, VA.

Green, A. and J.Z. Sasiadek (2004b). Dynamic and Trajectory Tracking Control of a Two-Link Flexible Robot Manipulator, *Journal of* Vibration and Control, **10**, 1415-1440.

Green, A. and J.Z. Sasiadek (2004c). Sensor Location Effect on Flexible Robot Control. In: *Proceedings of the 4th International Workshop on Robot Motion and Control*, *RoMoCo'04,* Elesevier, Oxford.

Green A. and J.Z. Sasiadek (2005). Adaptive Control of a Flexible Robot Using Fuzzy Logic. *AIAA Journal of Guidance, Control and Dynamics*, **28**, 36-42.

Matlab 6, Simulink 4 (2001). Control Systems and Fuzzy Logic Toolboxes, Release 12, The Mathworks, Inc., Natick, MA.

Sasiadek, J.Z. and R. Srinivasan (1989). Dynamic Modeling and Adaptive Control of a Single-Link Flexible Manipulator. *AIAA Journal of Guidance,Control and Dynamics*, **12**, 838-844.

Stieber, M. E., Vukovich, G., and E. Petriu (1997). Stability Aspects of Vision-Based Control for Space Robots. In: *Proceedings of the IEEE International Conference on Robotics and Automation*, IEEE Press, Piscataway, NJ, 2771-2776.

Thomson, W.T (1981). *Theory of Vibration with Applications*, (2nd Ed), Prentice-Hall, Upper Saddle River, NJ.

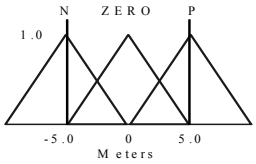

Fig. 2. MFs for Input Variables δ_1 and δ_2.

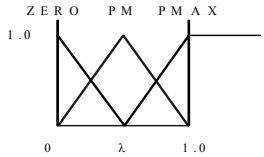

Fig. 3. MFs for Output Variableλ.

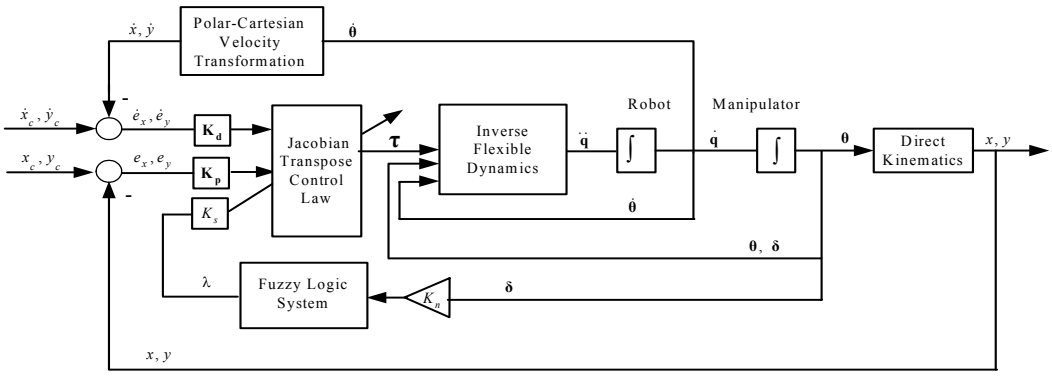

Fig. 4. FLS Adaptive Control Strategy.

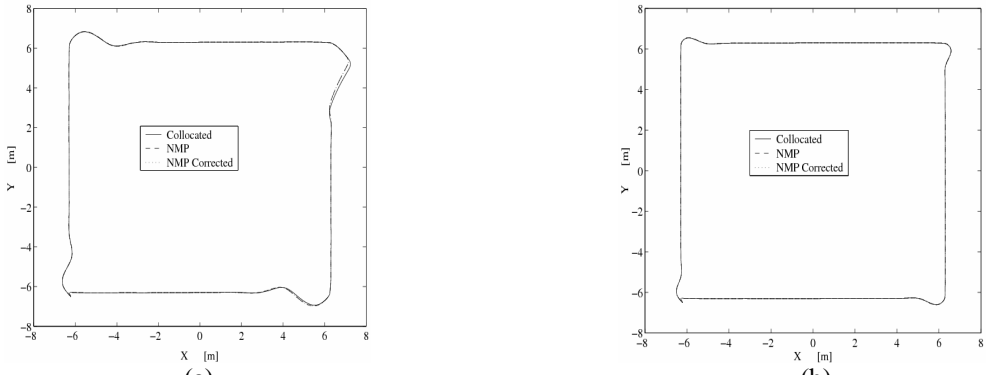

(a) (b)

Fig. 5 (a). Nonadaptive control with sensor collocated, noncollocated (NMP) at the end effector and NMP corrected, (b). Adaptive control with sensor collocated, noncollocated (NMP) at the end effector and NMP corrected.

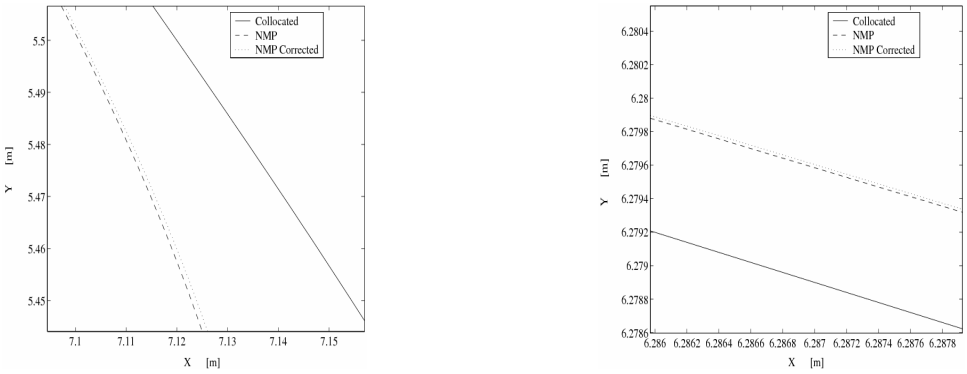

(a) (b)

Fig. 6 (a). Nonadaptive control with sensor collocated, noncollocated (NMP) at the end effector and NMP corrected (second direction switch zoomed), (b). Adaptive control with sensor collocated, noncollocated (NMP) at the end effector and NMP corrected (first direction switch zoomed).

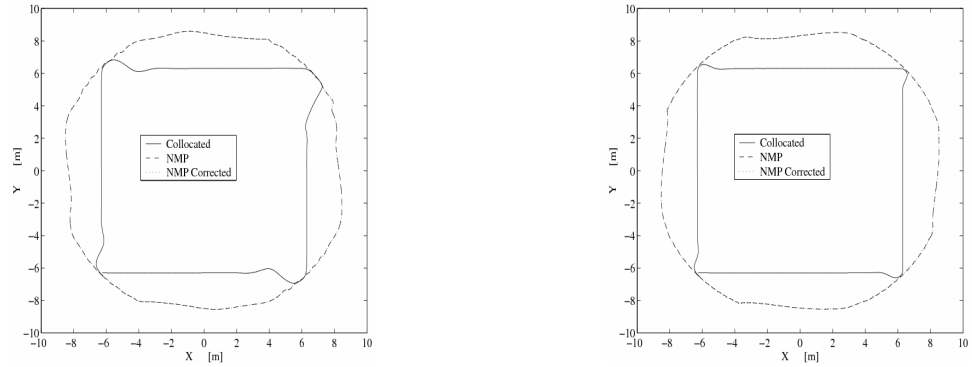

(a) (b)

Fig. 7 (a). Nonadaptive control with sensor collocated, noncollocated (NMP) at 2.25m on link 2 and NMP corrected, (b). Adaptive control with sensor collocated, noncollocated (NMP) at 2.25m on link 2 and NMP corrected.

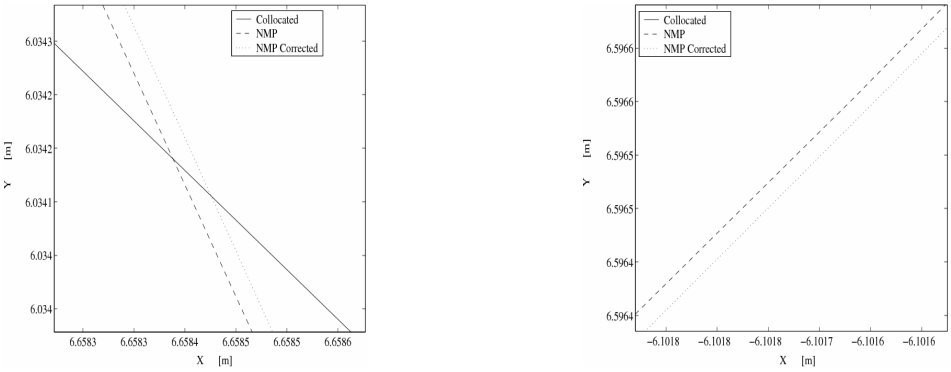

(a) (b)

Fig. 8 (a). Nonadaptive control with sensor collocated, noncollocated (NMP) at 2.25m on link 2 and NMP corrected (second direction switch zoomed), (b). Adaptive control with sensor collocated, noncollocated (NMP) at 2.25m on link 2 and NMP corrected (third direction switch zoomed).